厚生労働科学研究費補助金

難病・がん等の疾患分野の医療の実用化研究事業（再生医療関係研究分野）

分担研究報告書

ヒトiPS細胞から神経前駆細胞への誘導法の検討

研究分担者　神山淳　慶應義塾大学医学部　生理学教室　特任講師

【研究要旨】

本研究は、ヒト iPS 細胞から神経前駆細胞への分化誘導法を検討し、至適化を行なった。従来汎用される iPS 細胞から神経前駆細胞への分化誘導法(ニューロスフェア法)とは異なる単層培養系を利用した神経誘導法を利用し、再生医療用 iPS 細胞ストックにおける神経誘導能の検討及び安定培養に向けた培養法の検討を行った。さらに、予備的検討として単層系 hiPS-NPC を用いて免疫不全動物に移植を行ない、造腫瘍性の検討を行った。

A．研究目的

神経幹細胞の発見は従来不治の病であった中枢神経系における変性疾患や損傷に対する細胞治療への一つ可能性を提唱した。しかし、成体における神経幹細胞は採取が困難であり、研究レベルでは中絶胎児由来の神経幹細胞を用い、実験動物モデルにおける細胞治療の有用性が報告されてきた。しかしながら、治療用神経前駆細胞の供給源として想定された胎児由来神経前駆細胞やヒト ES 細胞由来神経前駆細胞は倫理的な問題が伴い、現実的ではない。京都大学の山中博士らにより開発された iPS 細胞樹立法は成体のヒト線維芽細胞や血球細胞からの樹立が可能であり、採取や樹立に伴う倫理的な問題がなく、有用なソースであることが期待されてきた。本研究では再生医療実現拠点ネットワーク事業再生医療実現拠点ネットワークプログラムにおける中核拠点『iPS 細胞研究中核拠点』より提供される再生医療用 iPS 細胞ストックを用い、神経前駆細胞へと分化誘導を行ない、再生医療用の iPS 細胞由来神経前駆細胞ストック構築に向けた分化誘導法の最適化及び妥当性を検討することを目的としている。中核拠点からの再生医療用 iPS 細胞ストックの提供時期は平成 26 年度後半が予定されているため、本年度は中核拠点より提供された再生医療用 iPS 細胞ストックと同様の手法で樹立された血球系由来 iPS 細胞株を利用し、分化誘導法の検討を行った。また、接着系培

養法の妥当性を検討するため、既報の論文により他研究室において樹立された単層培養系 hiPS-NPC を用いて造腫瘍性を検討した。

B．研究方法

1）iPS 細胞からの神経誘導法の検討

平成 26 年度後半に提供が予定されている再生医療用 iPS 細胞ストックを利用した神経誘導を行なう為のパイロットスタディを行なった。再生医療用 iPS 細胞ストックと同様の手法で樹立された iPS 細胞を iPS 細胞樹立中核拠点より入手し、神経誘導を試みた。

2）iPS 細胞由来神経前駆細胞の造腫瘍性の検討

既に他研究室により樹立された単層培養系 hiPS-NPC(lt-NES)を用いた解析を行った。hiPS-NPC にルシフェラーゼで標識後、免疫不全動物(NOD/SCID マウス)の脳へと移植した。IVIS システムにより移植細胞の増殖の程度を経時的に解析した。

(倫理面への配慮)

本研究は、慶應義塾大学倫理委員会で人権擁護、不利益・危険性の排除、説明と同意に関して十分な審査を経た承認のもとに行われる。ヘルシンキ宣言に基づく倫理的原則を遵守し、下記の各種指針にもとづいて研究計画を立案・遂行するものとする。

- ヒトゲノム・遺伝子解析研究に関する倫理指針
- その他（文部科学省研究振興局長通知 19 文科振第 852 号）

実験動物を使用する研究を含む研究計画：「動物の愛護及び管理に関する法律」および関連した指針に則って研究を行う。慶應義塾大学医学部では、動物実験委員会を設置し、関連法案および指針を遵守した審査が行われている。本研究に関する動物実験の多くは既に同委員会の承認を得ている。今後本研究を遂行する上で、新たな課題の必要が出てきた場合は、同委員会に申請し、承認を得るものとする。

ヒト細胞を用いた基礎研究計画：ヒト神経堤由来幹細胞を用いた脊髄再生研究、ヒト ES 細胞の使用研究、ヒト iPS 細胞樹立等の基礎研究について、ヒト細胞入手法を含めて機関内倫理委員会（慶應義塾大学医学部の倫理委員会）の承認を得ている。今後本研究を遂行する上で、必要に応じて同委員会に申請を行い、承認を得るものとする。尚、同委員会では、法令違反を行った場合等に備えて、臨時委員会を緊急に開催するなどの処置により、当該研究を中止することが出来る。

C. 研究結果

1）iPS 細胞からの神経誘導法の検討

ヒトiPS細胞から単層培養系への誘導法は既報が存在するものの（Falk et al., PloS One 2012)、iPS細胞樹立中核拠点から提供されるiPS細胞と同等の細胞(血液細胞)から樹立されたiPS細胞では神経誘導能が検討されていなかった。そこで先ず、神経誘導を検討した。その結果誘導後２週間程度で神経ロゼット様構造を呈する細胞集団が見出された。さらに、PLZF, ZO1, DACH1等の神経ロゼット選択的マーカーの発現も観察された(図１)。

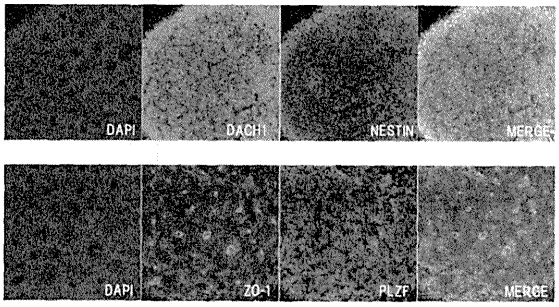

図１

次にロゼット構造を形成する細胞群を分離・回収し、接着性の基質状での培養系へと移行した。このような手法で誘導した単層培養系hiPS-NPCは神経前駆細胞マーカー(Sox1,Sox2, Nestin)を発現しており(図２)、分化誘導によりニューロンへの分化能が確認された。iPS細胞樹立中核拠点より提供された２つのiPS細胞株で同様の現象が確認されたため、本手法はiPS細胞から神経前駆細胞への分化系として有用であることが推察された。

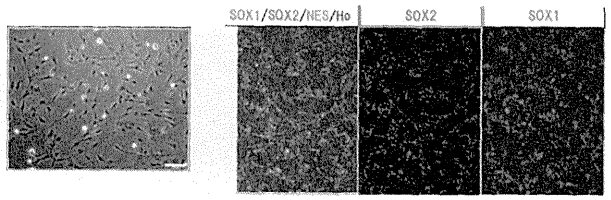

図２

2）hiPS-NPCの腫瘍原性の検討

他施設により樹立されたhiPS-NPC(lt-NES)をルシフェラーゼを発現するようにさせる為にレンチウイルスによりhiPS-NPCを標識し、免疫不全動物の脳内に移植した。細胞の増殖度を生きた個体において経時的に解析した結果、hiPS-NPCは図に示すような増殖曲線を描いた(図３)。

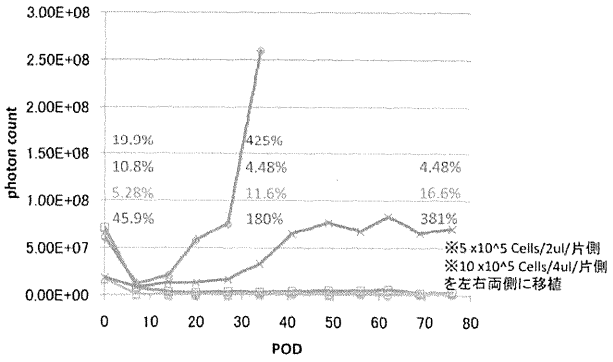

図３

既報では腫瘍形成能を示さないことが報告されていたため(Fujimoto et al., Stem Cells)、hiPS-NPCの腫瘍原性を検討するため組織学的な解析をし、移植細胞がニューロンへと分化していることが明らかとなったが（図４)、移植部位以外へ細胞が播種しており、脳室内での細胞増殖が観察された。

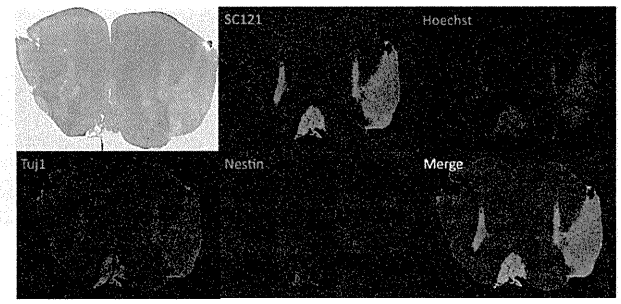

図４

D．考察

血液細胞由来のiPS細胞においても線維芽細胞由来iPS細胞と同様に神経幹細胞へと分化誘導可能であることが明らかとなった。単層培養系であり、通常の細胞培養時に個々の細胞の形態学的変化を把握可能であるため細胞の急激な状態変化を把握可能な系であると考えられた。現有する２つのiPS細胞株において同様に神経前駆細胞の誘導が可能であり、安定して神経前駆細胞を樹立可能であったためiPS-NPC樹立という観点から標準プロトコールになる可能性を秘めていると考えられた。また、樹立したhiPS-NPCはほぼ均一に神経前駆細胞マーカーを発現していたため、細胞種としての不均一性の問題は考慮する必要がなく、造腫瘍性という観点からの不均一性のみに着目可能であると考えられた。また、単層培養系で他研究室において樹立されたhiPS-NPCはニューロンへの分化能が認められたものの、移植後に増殖が見られ、また移植部位以外にも生着及び播種していることが認められたため、腫瘍原性を有している可能性が考えられた。この点に関しては現在神経病理学的な見地から検討中である。

E．結論

iPS細胞-NSPCにおける造腫瘍性の実体解明には単一細胞由来のNPCの樹立が必須であり、本研究では再生医療用iPS細胞ストックを利用し作製されたhiPS-NPCの造腫瘍性の実体解明に向けた基礎的な基盤が確立されたもの考えており、これらをもとに腫瘍原性を事前に検出可能な腫瘍マーカーの同定が期待される。

F．健康危険情報

特になし。

G．研究発表

（１）論文発表

1. Zhou Z, Kohda K, Ibata K, **Kohyama J**, Akamatsu W, Yuzaki M, Okano HJ, Sasaki E, Okano H.: Reprogramming non-human primate somatic cells into functional neuronal cells by defined factors. **Mol Brain.** 7(1):24. 2014

2. Iwanami A, Gini B, Zanca C, Matsutani T, Assuncao A, Nael A, Dang J, Yang H, Zhu S, Kohyama J, Kitabayashi I, Cavenee WK, Cloughesy TF, Furnari FB, Nakamura M, Toyama Y, Okano H, Mischel PS.: PML

mediates glioblastoma resistance to mammalian target of rapamycin (mTOR)-targeted therapies. **Proc Natl Acad Sci U S A.** 12;110(11):4339-4344 2013

3. Urayama S, Semi K, Sanosaka T, Hori Y, Namihira M, **Kohyama J**, Takizawa T, Nakashima K.: Chromatin accessibility at a STAT3 target site is altered prior to astrocyte differentiation.: Cell Struct Funct. 38(1):55-66, 2013

H．知的財産権の出願・登録状況
（予定を含む。）

特になし

III. 研究成果の刊行に関する一覧表

Ⅲ　研究成果の刊行に関する一覧表

書籍

著者氏名	論文タイトル名	書籍全体の編集者名	書　籍　名	出版社名	出版地	出版年	ページ
なし							

雑誌

発表者氏名	論文タイトル名	発表誌名	巻号	ページ	出版年
Nishimura S, Yasuda A, Iwai H, Takano M, Kobayashi Y, Nori S, Tsuji O, Fujiyoshi K, Ebise H, Toyama Y, Okano H, Nakamura M.	Time-dependent changes in the microenvironment of injured spinal cord affects the therapeutic potential of neural stem cell transplantation for spinal cord injury.	Mol Brain	6	3	2013
Takano M, Komaki Y, Hikishima K, Konomi T, Fujiyoshi K, Tsuji O, Toyama Y, Okano H, Nakamura M.	In vivo tracing of neural tracts in tip-toewalking Yoshimura mice by diffusion tensor tractography.	Spine	38	E66-72	2013

Shinozaki M, Yasuda A, Nori S, Saito N, Toyama Y, Okano H, Nakamura M.	Novel method for analyzing locomotor ability after spinal cord injury in Rats: Technical Note.	Neurologia medico-chirurgica	53	907-913	2013
Shinozaki M, Nakamura M, Konomi T, Kobayashi Y, Takano M, Saito N, Toyama Y, Okano H.	Distinct roles of endogenous vascular endothelial factor receptor 1 and 2 in neural protection after spinal cord injury.	Neurosci Res	78	55-64,	2014
Takano M, Kawabata S, Komaki Y, Shibata S, Hikishima K, Toyama Y, Okano H, Nakamura M.	Inflammatory cascades mediate synapse elimination in spinal cord compression.	J Neuro-inflammation	11	40	2014
Zhang L, Kaneko S, Kikuchi K, Sano A, Maeda M, Kishino A, Shibata S, Mukaino M, Toyama Y, Liu M, Kimura T, Okano H, Nakamura M.	Rewiring of regenerated axons by combining treadmill training with semaphorin3A inhibition.	Mol Brain	7(1)	14	2014
Iwai H, Nori S, Nishimura S, Yasuda A, Takano O, Fujiyoshi K, Toyama Y, Okano H, Nakamura M.	Transplantation of neural stem/ progenitor cells at different locations inmice with spinal cord injury.	Cell Transplant			2014 (in press)

Okano H, Nakamura M, Yoshida K, Okada Y, Tsuji O, Nori S, Ikeda E, Yamanaka S, Miura K.	Steps toward safe cell therapy using induced pluripotent stem cells.	Circulation Research	112	523-533	2013
Nakamura M, Okano H.	Cell transplantation therapies for spinal cord injury focusing on induced pluripotent stem cells.	Cell Research	23	70-80	2013
Matsui T, Akamatsu W, Nakamura M, Okano H.	Regeneration of the damaged central nervous system through rogramming technology: basic concepts and potential application for cell replacement therapy.	Exp Neurol			2014 (in press)
辻収彦, 海苔聡, 中村雅也	iPS細胞を用いた脊髄損傷治療の開発.	BIO Clinica	28	1208-1212	2013
中村雅也, 岡野栄之, 戸山芳昭	iPS細胞を用いた脊髄再生医療の展望 –基礎から臨床へ-.	日本内科学会誌	102	2247-2253	2013
中村雅也, 岡野栄之, 戸山芳昭	iPS細胞を使う－神経の研究へ.	整形外科	64	1311-1315	2013

Qin Y, Fu M, Takahashi M, Iwanami A, Kuga D, Rao RG, Sudhakar D, Huang T, Kiyohara M, Torres K, Dillard C, Inagaki A, Kasahara N, Goodglick L, Braun J, Mischel PS, Gordon LK, Wadehra M.	Epithelial membrane protein-2 (emp2) activates src and is a novel therapeutic target for gbm.	The Journal of biological chemistry.			2014
Read RD, Fenton TR, Gomez GG, Wykosky J, VandenbergSR, Babic I, Iwanami A, Yang H, Cavenee WK, Mischel PS, Furnari FB, Thomas JB.	A kinome-wide rnai screen in drosophila glia reveals that the rio kinases mediate cell proliferation and survival through torc2-akt signaling in glioblastoma.	PLoS genetics	9	e1003253	2013
Masui K, Tanaka K, Akhavan D, Babic I, Gini B, Matsutani T, Iwanami A, Liu F, Villa GR, Gu Y, Campos C, Zhu S, Yang H, Yong WH, Cloughesy TF, Mellinghoff IK, Cavenee WK, Shaw RJ, Mischel PS.	Mtor complex 2 controls glycolytic metabolism in glioblastoma through foxo acetylation and upregulation of c-myc.	Cell metabolism.	18	726-739	2013

Iwanami A, Gini B, Zanca C, Matsutani T, Assuncao A, Nael A, Dang J, Yang H, Zhu S, Kohyama J, Kitabayashi I, Cavenee WK, Cloughesy TF, Furnari FB, Nakamura M, Toyama Y, Okano H, Mischel PS.	Pml mediates gliobl astoma resistance to mammalian target of rapamycin (mtor) -targeted therapies.	Proc Natl Acad Sci USA	110	4339-4344	2013
Iwanami A, Cloughesy TF, Cavenee WK, Mischel PS.	Arsenic reverses gli oblastoma resistance to mtor-targeted th erapies.	Cell Cycle.			2013
Zhou Z, Kohda K, Ibata K, Kohyama J, Akamatsu W, Yuzaki M, Okano HJ, Sasaki E, Okano H.	Reprogramming non -human primate so matic cells into fun ctional neuronal cell s by defined factors	Mol Brain	7	(1):24	2014
Urayama S, Semi K, Sanosaka T, Hori Y, Namihira M, Kohyama J, Takizawa T, Nakashima K.	Chromatin accessibil ity at a STAT3 tar get site is altered p rior to astrocyte dif ferentiation	Cell Struct Fu nct.	38(1):	55-66,	2013

IV. 研究成果の刊行物・別刷

Molecular Brain

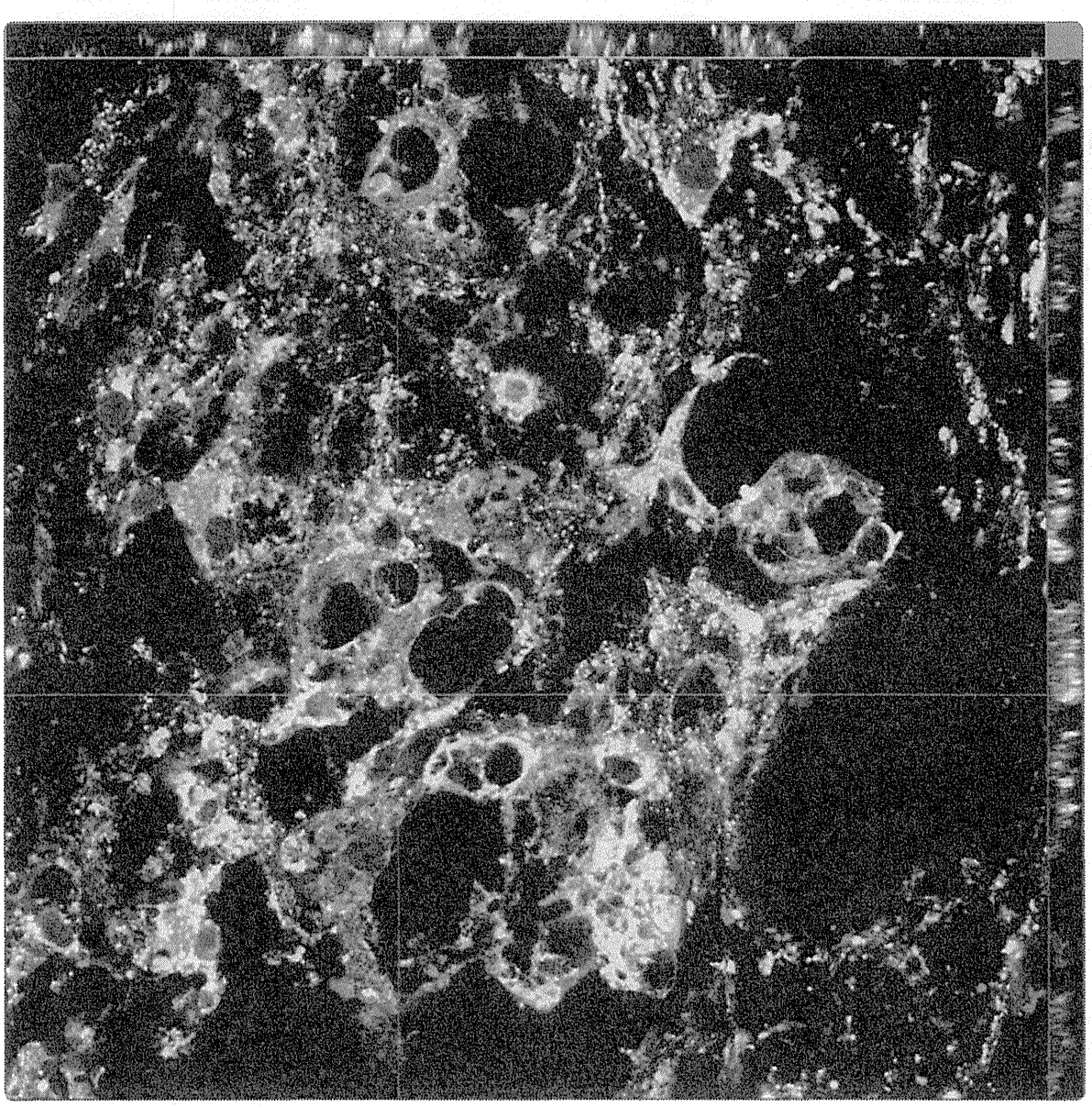

Time-dependent changes in the microenvironment of injured spinal cord affects the therapeutic potential of neural stem cell transplantation for spinal cord injury

Nishimura *et al.*

BioMed Central

Nishimura *et al. Molecular Brain* 2013, **6**:3
http://www.molecularbrain.com/content/6/1/3

Nishimura et al. Molecular Brain 2013, 6:3
http://www.molecularbrain.com/content/6/1/3

Molecular Brain

RESEARCH Open Access

Time-dependent changes in the microenvironment of injured spinal cord affects the therapeutic potential of neural stem cell transplantation for spinal cord injury

Soraya Nishimura[1,2], Akimasa Yasuda[1], Hiroki Iwai[1,2], Morito Takano[1,2], Yoshiomi Kobayashi[1,2], Satoshi Nori[1], Osahiko Tsuji[3], Kanehiro Fujiyoshi[4], Hayao Ebise[5], Yoshiaki Toyama[1], Hideyuki Okano[2*] and Masaya Nakamura[1*]

Abstract

Background: The transplantation of neural stem/progenitor cells (NS/PCs) at the sub-acute phase of spinal cord injury, but not at the chronic phase, can promote functional recovery. However, the reasons for this difference and whether it involves the survival and/or fate of grafted cells under these two conditions remain unclear. To address this question, NS/PC transplantation was performed after contusive spinal cord injury in adult mice at the sub-acute and chronic phases.

Results: Quantitative analyses using bio-imaging, which can noninvasively detect surviving grafted cells in living animals, revealed no significant difference in the survival rate of grafted cells between the sub-acute and chronic transplantation groups. Additionally, immunohistology revealed no significant difference in the differentiation phenotypes of grafted cells between the two groups. Microarray analysis revealed no significant differences in the expression of genes encoding inflammatory cytokines or growth factors, which affect the survival and/or fate of grafted cells, in the injured spinal cord between the sub-acute and chronic phases. By contrast, the distribution of chronically grafted NS/PCs was restricted compared to NS/PCs grafted at the sub-acute phase because a more prominent glial scar located around the lesion epicenter enclosed the grafted cells. Furthermore, microarray and histological analysis revealed that the infiltration of macrophages, especially M2 macrophages, which have anti-inflammatory role, was significantly higher at the sub-acute phase than the chronic phase. Ultimately, NS/PCs that were transplanted in the sub-acute phase, but not the chronic phase, promoted functional recovery compared with the vehicle control group.

Conclusions: The extent of glial scar formation and the characteristics of inflammation is the most remarkable difference in the injured spinal cord microenvironment between the sub-acute and chronic phases. To achieve functional recovery by NS/PC transplantation in cases at the chronic phase, modification of the microenvironment of the injured spinal cord focusing on glial scar formation and inflammatory phenotype should be considered.

Keywords: Spinal cord injury, Neural stem/progenitor cells, Cell transplantation, Chronic phase, Microenvironment

* Correspondence: hidokano@a2.keio.jp; masa@a8.keio.jp
[2]Department of Physiology, Keio University School of Medicine, 35 Shinanomachi, Shinjuku, Tokyo 160-8582, Japan
[1]Department of Orthopaedic Surgery, 35 Shinanomachi, Shinjuku, Tokyo 160-8582, Japan
Full list of author information is available at the end of the article

Background

The injured spinal cord exhibits little spontaneous recovery and, as a result, many spinal cord injury (SCI) patients suffer from permanent functional impairments, such as motor and sensory dysfunction, and bladder and rectal disturbance. However, some previous reports have shown that neural stem/progenitor cells (NS/PCs) transplanted into the injured spinal cord of rodents [1-6] and non-human primates [7], 7–10 days post-injury (DPI), promote functional recovery after SCI. These reports indicate that NS/PC transplantation has therapeutic potential for SCI when performed during the sub-acute phase. However, patients continue to seek new therapies for SCI many years after their original injury, and most are therefore in the chronic phase. Although many researchers have sought to achieve functional recovery at the chronic phase of SCI by NS/PC transplantation, with one exception [8], no significant recovery of motor function has been obtained in animal models of chronic-phase SCI [9-12]. Despite differences in the survival rate, the cell types derived from the grafted NS/PCs and the distribution of grafted cells transplanted at the sub-acute versus the chronic phase remain unknown. Thus, it remains unanswered as to why grafted NS/PCs do not exert therapeutic benefits in the injured spinal cord at the chronic phase. To address this question, this study analyzed fetus-derived NS/PCs transplanted into the injured spinal cord of mice at 9 DPI and 42 DPI.

To assess the survival rate of grafted cells, we performed quantitative analysis using bioluminescence imaging (BLI) on a weekly basis until 42 days after transplantation. BLI is a powerful tool for the detection of exclusively living grafted cells that stably express luciferase in living animals after administration of luciferin, the luciferase substrate, because the luciferin-luciferase reaction depends on oxygen and ATP [13]. In this study, no significant difference in the survival rate of grafted cells between the sub-acute and chronic transplanted (TP) groups was observed at each experimental time point. Immunohistology also revealed no significant difference in the differentiation pattern of grafted NS/PCs between the two groups. In addition, inflammatory cytokines and growth factors, which influence the survival rate and differentiation characteristics of grafted cells, were expressed at similar levels at both phases. By contrast, the grafted cells were distributed broadly from the epicenter to rostral and caudal sites in the sub-acute TP group, whereas they remained near the lesion epicenter, due to extensive glial scarring, in the chronic TP group. Moreover, prominent macrophages distributed at and around the lesion epicenter in the sub-acute phase by immunohistochemistry, and microarray analysis demonstrated that the expression of Arginase-1, which is associated with M2 macrophages, was up-regulated significantly at the sub-acute phase than the chronic phase. These findings indicated that the characteristics of post-SCI inflammation are different between the sub-acute and chronic phases.

Consequently, the grafted NS/PCs did not promote any motor functional or histological recovery in the chronic TP group, while the sub-acute TP group demonstrated significant recovery compared with the vehicle control group. Taken together, these data suggest that a combination therapy of NS/PC transplantation with control of glial scar formation or inflammatory reaction may be critical to achieving functional recovery for chronic SCI.

Results

In vitro characterization of transgenic mouse-derived NS/PCs that ubiquitously express fluorescent protein-fused luciferase (ffLuc)-cp156

To identify and monitor the grafted cells by bio-imaging, a transgenic mouse that ubiquitously expresses ffLuc-cp156 was previously developed [14]. NS/PCs derived from this transgenic mouse showed strong and stable emission of ffLuc-cp156 *in vitro* (Figure 1A, B). The number of NS/PCs and the photon counts measured by BLI were significantly correlated (Figure 1B, C).

We proceeded to perform differentiation and proliferation assays of these NS/PCs *in vitro*. The NS/PCs differentiated into βIII tubulin (Tuj-1)$^+$ neurons (21.0 ± 0.5%), glial fibrillary acidic protein (GFAP)$^+$ astrocytes (63.0 ± 1.5%), and 2'3'-cyclic nucleotide 3'-phosphodiesterase (CNPase)$^+$ oligodendrocytes (10.4 ± 0.5%) *in vitro* (Figure 1D, E). ATP production, an indirect measurement, was used to assess NS/PC proliferative ability [15]. The doubling time of the NS/PCs was 28.8 ± 0.8 h. The differentiation rate and proliferative ability of NS/PCs obtained from the transgenic mice were equivalent to those previously reported for wild-type NS/PCs [16,17].

Comparison of the injured spinal cord microenvironment between the sub-acute and chronic phases

To clarify differences in the microenvironment of the injured spinal cord between the sub-acute and chronic phases, histological analyses of spinal cord tissues at 9 DPI and 42 DPI were performed. Spinal cord atrophy and glial scar formation were more prominent at and around the lesion epicenter at 42 DPI than at 9 DPI (Figure 2A). A significantly larger CS56$^+$ chondroitin sulfate proteoglycan (CSPG) area was detected at the lesion site at 42 DPI than at 9 DPI (Figure 2A, B). Furthermore, Iba1$^+$ macrophages infiltrated area was more prominent at the lesion site at 9 DPI but not at 42 DPI (Figure 2A, C).

To analyze the gene expression profile in the injured spinal cord, we performed microarray analysis

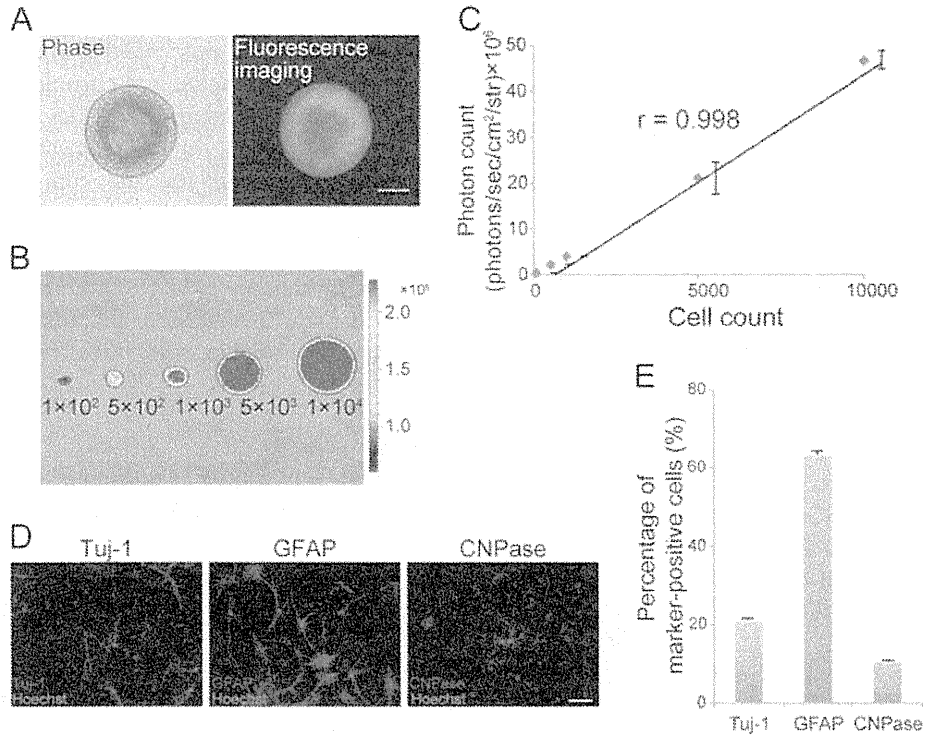

Figure 1 *In vitro* characterization of the NS/PCs derived from transgenic mice that ubiquitously express ffLuc-cp156. A, Fluorescence image showing NS/PCs derived from fetal transgenic mice expressing the fluorescent protein cp156-Venus, which is originally modified from GFP. **B**, Bioluminescent signals originating from the luciferase were detected in the NS/PCs by BLI. **C**, The number of NS/PCs was significantly correlated with the measured photon count by BLI. Values are means ± SEM (n = 3). **D**, Tertiary NS/PCs differentiated into Tuj-1$^+$ neurons, GFAP$^+$ astrocytes, and CNPase$^+$ oligodendrocytes *in vitro*. **E**, Quantitative analysis of Tuj-1$^+$ neurons, GFAP$^+$ astrocytes, and CNPase$^+$ oligodendrocytes *in vitro*. Values are means ± SEM (n = 5). Scale bar: 100 μm in (A) and 50 μm in (D).

to provide a global analysis of the gene expression profile of spinal cord tissues at 9 DPI and 42 DPI. As a control, samples of uninjured naïve spinal cord were prepared. Principal component analysis (PCA) of all the microarray data revealed that the samples of the intact, 9 DPI and 42 DPI groups were clustered at different locations (Figure 2D). Hierarchical clustering of the target genes, which were narrowed down by cut-off values for expression levels and by fold change, revealed that the gene expression profiles of both injured groups were dramatically different from that of the intact group. Furthermore, the gene expression pattern at 9 DPI was similar to that at 42 DPI, but the magnitude of changes in gene expression differed between the two injury groups. At 9 DPI, the magnitude of gene expression changed more remarkably than that at 42 DPI (Figure 2E).

Subsequently, we focused on individual gene expression levels. No significant differences were observed in the expression levels of genes for individual inflammatory cytokines or growth factors between the two injury groups (Figure 2F, G). By contrast, the expression of CD36 and CD68, which are expressed on monocytes and macrophages, was significantly elevated at 9 DPI (Figure 2H). These results were consistent with the immunostaining results for Iba1 (Figure 2A, C). Interestingly, the expression of arginase-1, which is associated with anti-inflammatory M2 macrophages, was also significantly higher at 9 DPI than at 42 DPI, whereas no significant differences were observed in the expression levels of genes associated with pro-inflammatory M1 macrophages, such as CD86 or inducible nitric oxide synthase (iNOS). Consistent with these findings, immunohistological analysis revealed more Iba1 and arginase-1 double-positive cells at 9 DPI (14.1 ± 1.5%) than at 42 DPI (0.9 ± 0.4%) (Figure 2I, J).

We also evaluated the phagocytic activity of the macrophages recruited into the injured spinal cord by performing immunohistochemistry for LAMP2, a marker for endosomes or lysosomes. At 9 DPI, substantial numbers of infiltrating Iba1, arginase-1, and LAMP2 triple-positive cells were observed at and near the lesion epicenter. In contrast, only a small amount of LAMP2-positive phagocytes were localized to the lesion epicenter at 42 DPI (Figure 2I). In addition, no significant expression of myeloperoxidase, a marker of neutrophils, was observed at either 9 DPI or 42 DPI (Figure 2H).

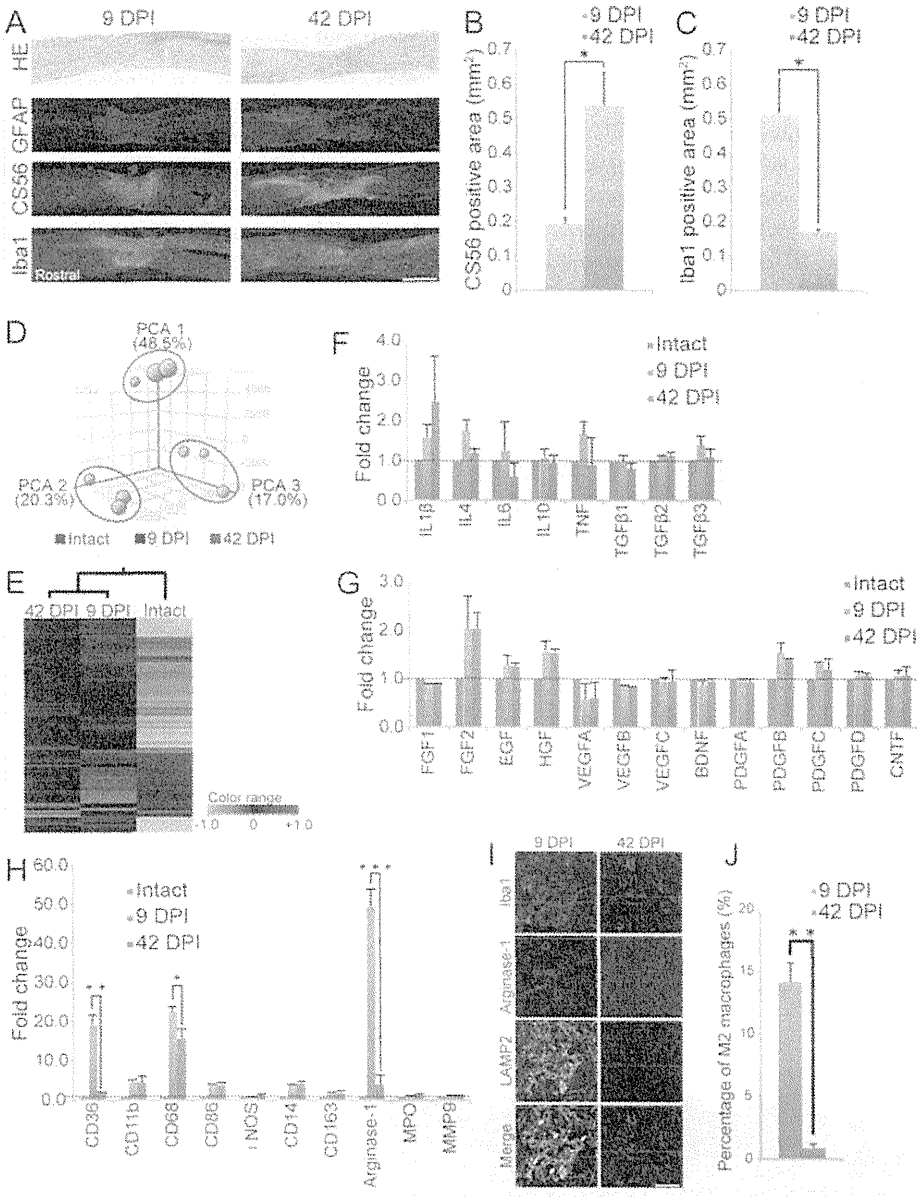

Figure 2 Comparison of the microenvironment of the injured spinal cord at 9 DPI versus 42 DPI. A, Representative images of HE staining and immunofluorescence staining for GFAP, CS56, and Iba1 in sagittal sections. **B**, CSPGs accumulation was more prominent at the lesion site at 42 DPI than at 9 DPI. Values are means ± SEM (n = 3). $^{*}P < 0.05$. **C**, More Iba1-positive cells were distributed at the lesion site at 9 DPI than at 42 DPI. Values are means ± SEM (n = 3). $^{*}P < 0.05$. **D**, Overview of all the microarray data by PCA. The samples of each group were clustered at different locations on 3D visualization. **E**, Hierarchical clustering analysis showed that the gene expression pattern at 9 DPI was similar to that at 42 DPI. However, the magnitude of changes in gene expression differed between the two injury groups. Green tiles show downregulated genes and red tiles indicate upregulated genes. **F-H**, Gene expression signals of cytokines (**F**), growth factors (**G**), and markers of inflammatory cells (**H**) at 9 DPI and 42 DPI. The gene expression levels of markers associated with microglia/macrophages significantly differed between 9 DPI and 42 DPI, but those of all cytokines and growth factors did not. Data are the mean fold-change values versus intact samples. Values are means ± SEM (n = 3). $^{*}P < 0.05$, $^{**}P < 0.01$, $^{***}P < 0.001$. **I**, Representative images of immunofluorescence staining for Iba1, arginase-1, and LAMP2 in sagittal sections of the lesion epicenter at 9 DPI and 42 DPI. Arrows: Iba1^{+}/arginase-1^{+}/LAMP2^{+} triple-positive cells. **J**, At the lesion epicenter, more Iba1^{+}/arginase-1^{+} M2 macrophages had infiltrated at 9 DPI compared with 42 DPI. Values are means ± SEM (n = 3). $^{**}P < 0.01$. Scale bar: 1000 μm in (**A**) and 50 μm in (**J**).

Comparison of survival rates and differentiation phenotypes of the grafted NS/PCs between the sub-acute and chronic TP groups

BLI analysis only detects luminescent photon signals from living cells, and the number of NS/PCs and the photon count *in vitro* were significantly correlated. To investigate whether similar correlativity was observed *in vivo*, various numbers of NS/PCs (approximate range 2.5×10^4 to 5×10^5 cells) were transplanted into the intact spinal cord of mice (Figure 3A). These data revealed that the photon count was significantly proportional to the number of grafted cells *in vivo* (Figure 3B).

We next analyzed the survival rate of the grafted cells on a weekly basis until 42 days after transplantation using BLI (Figure 3C). At 7 days after transplantation, BLI analysis revealed that the survival of grafted cells was reduced to 12.4 ± 5.6% in the sub-acute TP group and to almost the same level in the chronic TP group (15.2 ± 2.9%). At 42 days after

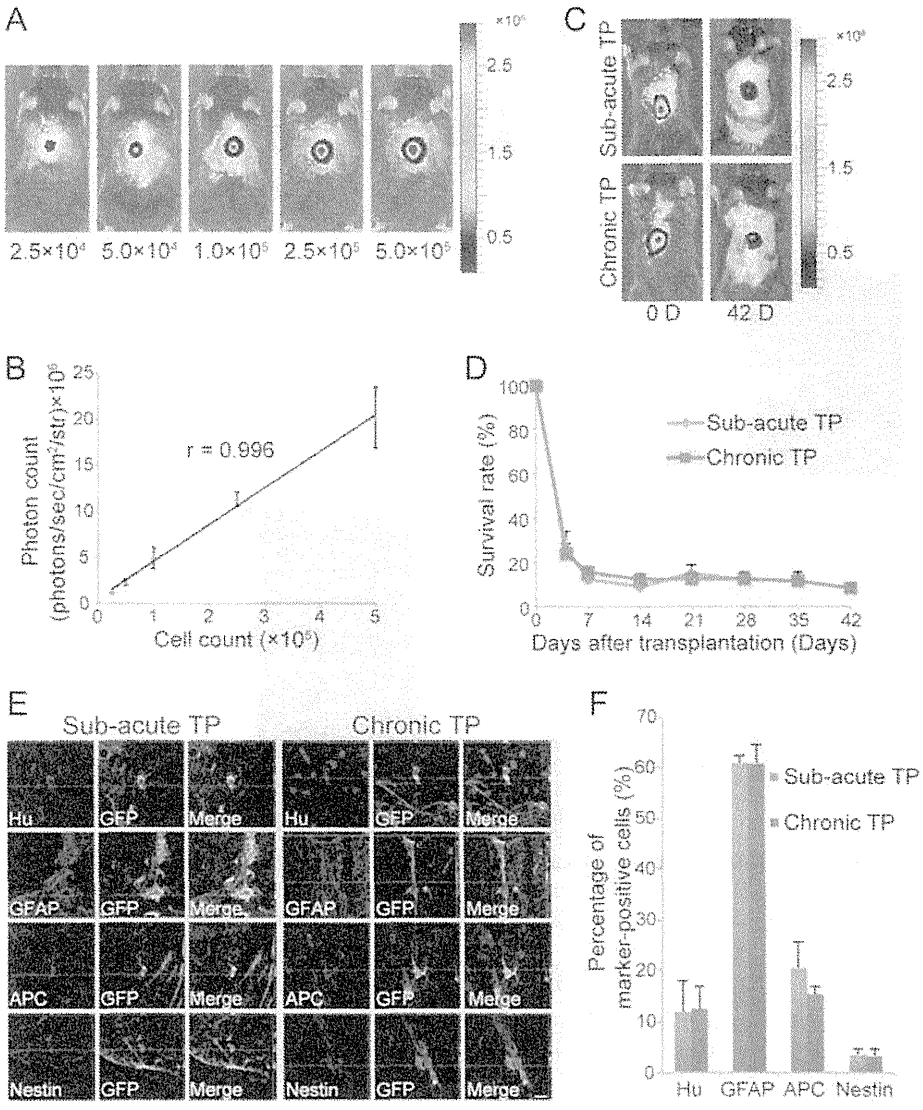

Figure 3 Survival rate and differentiation phenotype of grafted cells in the sub-acute and chronic TP groups. A, Representative *in vivo* BLI of naïve mice transplanted with various numbers of NS/PCs. **B**, The number of NS/PCs and the measured photon count were significantly correlated *in vivo*. Values are means ± SEM (n = 3). **C**, Representative *in vivo* BLI of the sub-acute and chronic TP groups immediately and 42 days after transplantation. **D**, Quantitative analysis using BLI revealed no significant difference in the survival rate of grafted cells between the sub-acute and chronic TP groups up to 42 days after transplantation. Values are means ± SEM (n = 10). **E**, GFP^+ grafted cells differentiated into Hu^+ neurons, $GFAP^+$ astrocytes, and APC^+ oligodendrocytes in the sub-acute and chronic TP groups. **F**, The differentiation rate of grafted cells into the three neural cell lineages did not significantly differ between the sub-acute and chronic TP groups 42 days after transplantation. Only a small number of $nestin^+$ neural progenitor cells was detected in the sub-acute and chronic TP groups. Values are means ± SEM (n = 3). Scale bar: 10 μm in (C).

transplantation, approximately 8% of the cells survived in both the sub-acute and chronic groups (8.6 ± 2.6% vs. 8.3 ± 1.9%). The survival rate of grafted cells did not significantly differ between the sub-acute and chronic TP groups at any time point examined (Figure 3D).

To evaluate the differentiation phenotype of the grafted cells *in vivo*, immunostaining for cell markers was performed 42 days after transplantation for both the sub-acute and chronic groups. Green fluorescent protein $(GFP)^+$ grafted cells differentiated into all three neural lineages in both groups (Figure 3E). Quantitative analyses revealed that in the sub-acute and chronic TP groups, most of the grafted cells differentiated into $GFAP^+$ astrocytes (60.8 ± 1.6% and 60.7 ± 3.7%), followed by adenomatous polyposis coli antigen $(APC)^+$ oligodendrocytes (20.3 ± 5.1% and 15.3 ± 1.3%) and Hu^+ neurons (11.8 ± 6.0% and 12.4 ± 4.2%). The differentiation rates of neurons, astrocytes, and oligodendrocytes did not significantly differ between the sub-acute and chronic TP groups (Figure 3F). Nestin-positive cells represented around 3% of the grafted cells in both TP groups.

Grafted cells were limited to the lesion epicenter in the chronic TP group due to extensive glial scar formation

To examine whether the prominent glial scarring seen in the chronic TP group affected the distribution of grafted cells, we performed immunostaining for GFP in both TP groups. In sagittal sections of the sub-acute TP group, GFP^+ grafted cells were found at the epicenter and at rostral and caudal sites, whereas in the chronic TP group, grafted cells were seen almost exclusively at the lesion epicenter (Figure 4A, B). Quantitative analysis of the GFP^+ areas in the axial sections revealed that the GFP^+ area in the sub-acute TP group, which spread from 3 mm rostral to 2 mm caudal from the lesion epicenter, was significantly larger than that in the chronic TP group (Figure 4C). Moreover, to clarify what causes the difference of distribution of grafted cells, double immunostaining for GFP and CS56 was performed in both TP groups. The GFP^+ grafted cells were surrounded and enclosed by $CS56^+$ CSPG areas at the lesion site in the chronic TP group, whereas the grafted cells distributed beyond CSPGs areas due to less accumulation of CSPG around the lesion site in the sub-acute TP group (Figure 4D, E).

NS/PC transplantation at the sub-acute phase, but not at the chronic phase, contributes to the preservation and/or enhancement of myelination and axonal growth

To compare the effects of NS/PC transplantation on the injured spinal cord between the sub-acute and chronic groups, axial sections were examined histologically using hematoxylin-eosin (HE) staining (Figure 5A). In sections

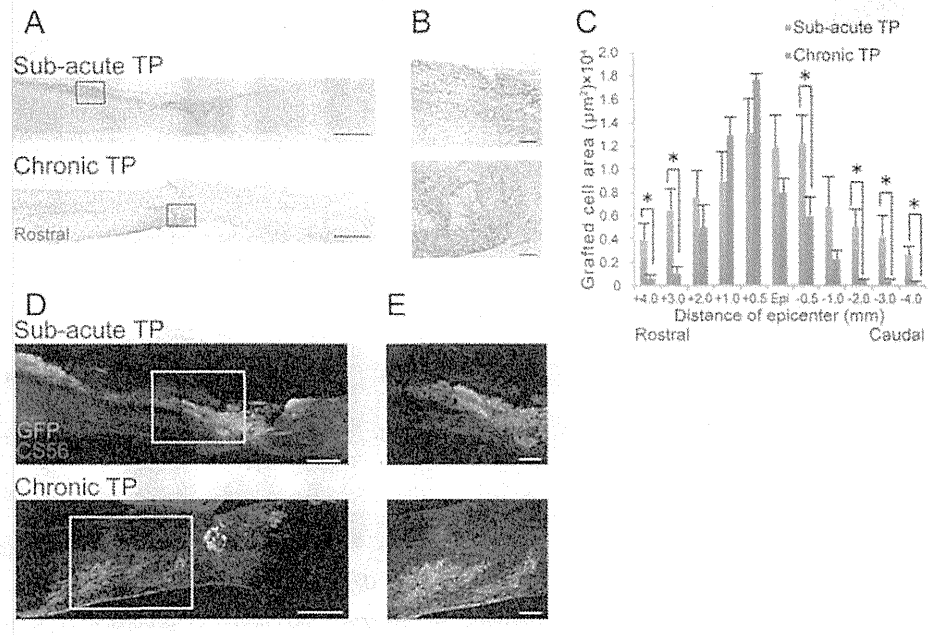

Figure 4 Distribution of grafted cells in the sub-acute and chronic TP groups. **A**, Representative images of GFP-immunostained sagittal sections in the sub-acute and chronic TP groups 42 days after transplantation. **B**, Higher-magnification images of the boxed areas in (**A**). **C**, Quantitative analysis of the GFP^+ grafted cell area in axial sections 42 days after transplantation. Grafted cells were located at the epicenter, rostral, and caudal sites in the sub-acute TP group, whereas they were limited to the lesion epicenter in the chronic TP group. Values are means ± SEM (n = 4). $^*P < 0.05$. **D**, Representative images of GFP- and CS56-immunostained sagittal sections from the sub-acute and chronic TP groups. **E**, Higher-magnification images of the boxed area in (**D**). In the sub-acute TP group, the GFP^+ grafted cells migrated away from the graft site due to less accumulation of $CS56^+$ CSPG around the lesion site, while the robust CSPGs prevented further migration of the grafted cells in the chronic TP group. Scale bar: 1000 μm in (**A**), 100 μm in (**B**), 500 μm in (**D**) and 200 μm in (**E**).

at the lesion epicenter and 4 mm rostral and caudal to it, the HE-stained images revealed significant atrophy of the spinal cord in the sub-acute phosphate-buffered saline (PBS) group compared to the sub-acute TP group. However, the experimental transverse area of the spinal cord did not significantly differ between the chronic TP and PBS groups (Figure 5B). In addition, the sub-acute TP group demonstrated a significantly larger myelinated area compared to the sub-acute PBS group at the lesion epicenter and in sections 4 mm rostral and caudal to the epicenter (Figure 5A), whereas the myelinated area did not significantly differ between the chronic TP and PBS groups (Figure 5C).

Next, to investigate axonal growth after NS/PC transplantation, immunostaining for 200 kDa neurofilament (NF-H) and 5-hydroxytryptamine (5HT) was performed in all experimental groups (Figure 5D). The NF-H$^+$ areas at the lesion site as well 4 mm rostral and caudal to it significantly differed between the sub-acute TP group and the other groups (Figure 5E). Furthermore, the sub-acute TP group demonstrated a significantly larger area of 5HT$^+$ serotonergic fibers in the distal cord compared to the other three groups (Figure 5F). By contrast, the chronic TP group demonstrated no significant differences in the NF-H$^+$ and 5HT$^+$ areas compared to the chronic PBS group.

NS/PC transplantation at the sub-acute phase, but not at the chronic phase, promotes motor function and electrophysiological recovery after SCI

Finally, we evaluated locomotor functional recovery by Basso Mouse Scale (BMS) score, Rotarod testing, and DigiGait. We confirmed that the mice exhibited complete paralysis of the hindlimbs by a BMS score of 0 at 1 DPI. At 7 DPI, the hind limb locomotor functions had recovered spontaneously to an approximate BMS score of 2, and plateaued at an approximate BMS score of 3, in all experimental groups except the sub-acute TP group. In the sub-acute TP group, significantly greater functional recovery was observed compared to the sub-acute PBS group at 14 DPI and thereafter. By contrast, the chronic TP group did not show any

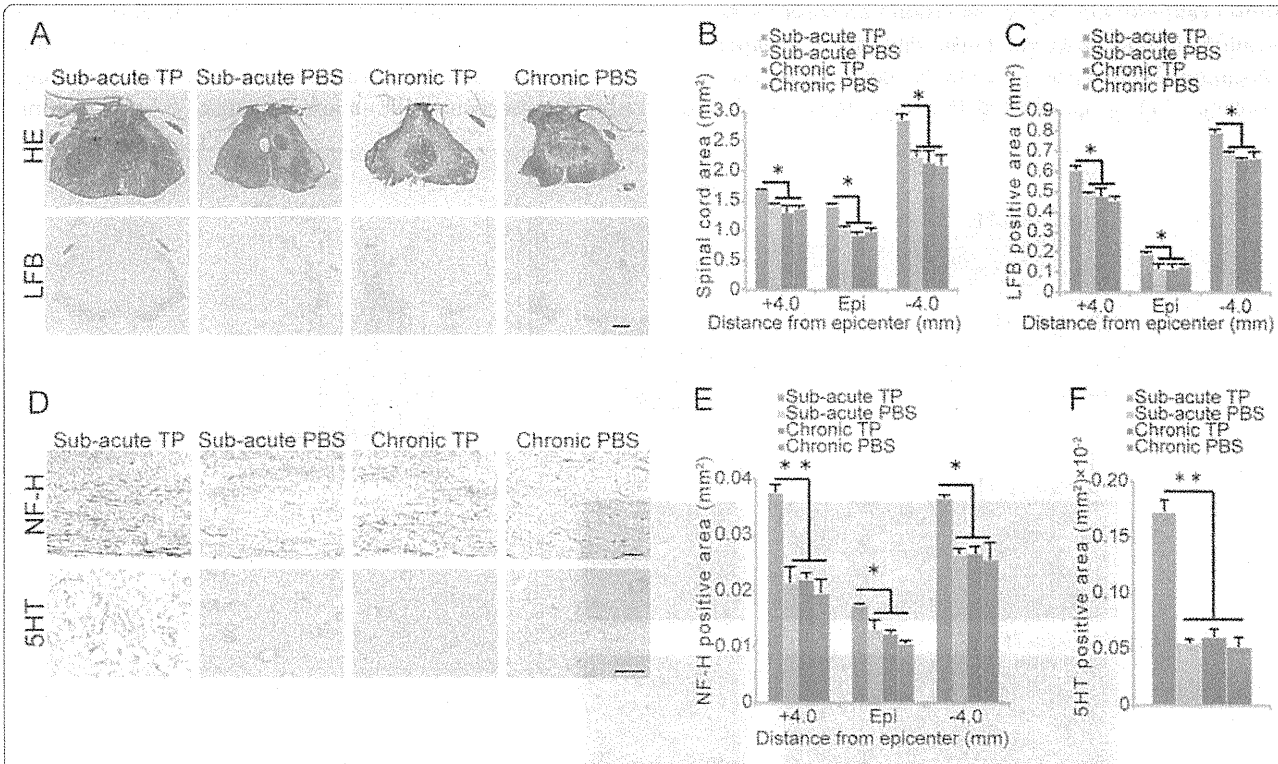

Figure 5 Comparison of the effects of NS/PC transplantation between the sub-acute and chronic TP groups. A, Representative HE- and LFB-stained images of axial sections at the lesion epicenter in the sub-acute TP, chronic TP, and both control groups. **B**, Significant atrophy of the spinal cords was observed in the chronic TP and control groups compared to that of the sub-acute TP group. Values are means ± SEM (n = 3). $^*P < 0.05$. **C**, The sub-acute TP group demonstrated a significantly larger myelinated area than the chronic TP and control groups. Values are means ± SEM (n = 3). $^*P < 0.05$. **D**, Representative images of sagittal sections stained for NF-H at the rim of the lesion epicenter and of axial sections stained for 5HT at the lumbar intumescence in the sub-acute TP, chronic TP, and each control group. **E**, Greater area of NF-H$^+$ neuronal fibers was observed in the sub-acute TP group than in the chronic TP group or control groups. Values are means ± SEM (n = 3). $^*P < 0.05$, $^{**}P < 0.01$. **F**, Significantly larger areas of 5HT$^+$ serotonergic fibers were detected in the sub-acute TP group than in the chronic TP or control groups. Values are means ± SEM (n = 3). $^{**}P < 0.01$. Scale bar: 100 μm in (**A**) and (**D**).